Physics Letters A 377 (2013) 1205–1209

Contents lists available at SciVerse ScienceDirect

Physics Letters A

www.elsevier.com/locate/pla

Mobility edge phenomenon in a Hubbard chain: A mean field study

Santanu K. Maiti [a,*], Abraham Nitzan [b]

[a] Physics and Applied Mathematics Unit, Indian Statistical Institute, 203 Barrackpore Trunk Road, Kolkata 700 108, India
[b] School of Chemistry, Tel Aviv University, Ramat-Aviv, Tel Aviv 69978, Israel

ARTICLE INFO

Article history:
Received 14 December 2012
Received in revised form 4 March 2013
Accepted 8 March 2013
Available online 15 March 2013
Communicated by R. Wu

Keywords:
Mobility edge
1D superlattice geometry
Mean field approach
Mesoscale switch

ABSTRACT

We show that a tight-binding one-dimensional chain composed of interacting and non-interacting atomic sites can exhibit multiple mobility edges at different values of carrier energy in presence of external electric field. Within a mean field Hartree–Fock approximation we numerically calculate two-terminal transport by using Green's function formalism. Several cases are analyzed depending on the arrangements of interacting and non-interacting atoms in the chain. The analysis may be helpful in designing mesoscale switching devices.

1. Introduction

Electronic localization phenomena in one-dimensional (1D) quantum systems have long been a central problem in condensed matter physics. It is well established that in infinite 1D systems with random site potentials, irrespective of the strength of randomness, all the energy eigenstates are exponentially localized [1]. Apart from this Anderson type localization another kind of localization known as Wannier–Stark localization is also observed in 1D materials, even in absence of any disorder, when the system is subjected to an external electric field [2]. For both cases, i.e., infinite 1D systems with random site potentials and 1D chains in presence of external electric field, one never encounters *mobility edges* separating the localized energy eigenstates from the extended ones, since all eigenstates are localized. However, there are some classes of 1D systems such as correlated disordered models, quasi-periodic Aubry–Andre model where several classic features of mobility edges at some specific values of energy are obtained [3–12]. Although the existence of such mobility edges in one- or two-dimensional systems has been described by several groups [10–15], a comprehensive study of this phenomenon is still lacking, particularly in the presence of electron–electron interaction. Still open fundamental questions are whether some special features exist in disordered 1D systems, or in the response of 1D systems to an externally applied electric field even in the presence of electron–electron interaction.

In the present Letter we investigate two-terminal electron transport through a 1D mesoscopic chain composed of interacting and non-interacting atomic sites in presence of external electric field. Although some works have been done in such superlattice structures [16–20], the analogous representation of metallic multilayered structures which exhibit several novel features [21–23], no rigorous effort has been made so far, to the best of our knowledge, to unravel the effect of the interplay of electron–electron interaction and an imposed external electric field on electron transport in such systems. Here we show that a traditional 1D lattice with electron–electron interaction, evaluated at the Hartree–Fock (HF) mean field (MF) level, is characterized by a mobility edge behavior at finite bias voltage. Furthermore, a superlattice structure comprising sites on which electron–electron interactions are expressed differently (some sites are interacting and some sites are non-interacting) is characterized by multiple occurrence of mobility edges at several values of the carrier energy. The applicability of mean field approximation in such superlattice geometries has already been reported in a recent work [24].

2. Model and calculation

We adopt a tight-binding (TB) framework to describe the model quantum system and numerically calculate two-terminal transport within a mean field Hartree–Fock approximation using a Green's function formalism. Several cases characterized by different arrangements of interacting and non-interacting atomic sites in the chain, are analyzed. For these models we calculate the average density of states (ADOS) and the two-terminal transmission probability, and find that sharp crossovers from completely opaque to

* Corresponding author. Fax: +91 33 2577 3026.
E-mail address: santanu.maiti@isical.ac.in (S.K. Maiti).

0375-9601/$ – see front matter
http://dx.doi.org/10.1016/j.physleta.2013.03.013

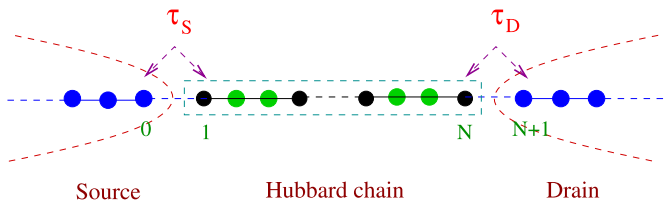

Fig. 1. (Color online.) A 1D mesoscopic chain, composed of interacting (filled black circle) and non-interacting (filled green circle) atomic sites, is attached to two semi-infinite 1D metallic electrodes, representing source and drain.

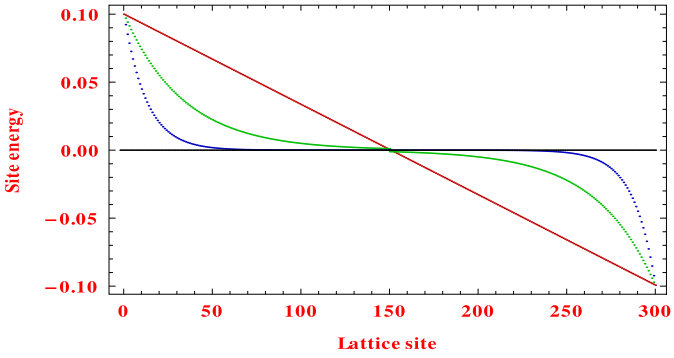

Fig. 2. (Color online.) Variation of voltage dependent site energies in a 1D chain with 300 lattice sites for three different electrostatic potential profiles when the bias voltage V is fixed at 0.2.

fully or partly transmitting zones take place at one or more specific electron energies. This observation suggests the possibility of controlling the transmission characteristics by gating the transmission zone, and using such superlattice structures as switching devices.

Let us refer to Fig. 1 where a 1D mesoscopic chain, composed of non-interacting and interacting atomic sites, is attached to two semi-infinite 1D non-interacting source and drain electrodes. In the arrangement of the two different atomic sites shown in Fig. 1, M ($M \geqslant 1$) non-interacting sites are placed between two interacting sites. Here and in what follows we make a restriction that interacting atoms are not placed successively. In a Wannier basis, the TB Hamiltonian for an N-site chain reads,

$$H_C = \sum_{i,\sigma} \epsilon_{i\sigma} c_{i\sigma}^{\dagger} c_{i\sigma} + \sum_{\langle ij\rangle,\sigma} t\left[c_{i\sigma}^{\dagger} c_{j\sigma} + c_{j\sigma}^{\dagger} c_{i\sigma}\right] + \sum_i U_i c_{i\uparrow}^{\dagger} c_{i\uparrow} c_{i\downarrow}^{\dagger} c_{i\downarrow} \tag{1}$$

where, $c_{i\sigma}^{\dagger}$ ($c_{i\sigma}$) is the creation (annihilation) operator of an electron at the site i with spin σ ($=\uparrow,\downarrow$), t is the nearest-neighbor hopping element, $\epsilon_{i\sigma}$ is the on-site energy of an electron at the site i of spin σ and U_i is the strength of on-site Coulomb interaction where $U_i = 0$ for the non-interacting sites. In presence of bias voltage V between the two electrodes an electric field is developed and the site energies become voltage dependent, $\epsilon_{i\sigma} = \epsilon_i^0 + \epsilon_i(V)$, where ϵ_i^0 is a voltage independent term. For the ordered chain ϵ_i^0 is a constant independent of i that can be chosen zero without loss of generality, while for the disordered case we select it randomly from a uniform "Box" distribution function in the range $-W/2$ to $W/2$.

The voltage dependence of $\epsilon_i(V)$ reflects the bare electric field in the bias junction as well as screening due to longer range e–e interaction not explicitly accounted for in Eq. (1). In the absence of such screening the electric field is uniform along the chain and $\epsilon_i(V) = V/2 - iV/(N+1)$. Below we consider this as well as screened electric field profiles, examples of which are shown in Fig. 2. We will see that the appearance of multiple mobility edges in superlattice geometries strongly depends on the existence of finite bias and on the profile of the bias drop along the chain.

The Hamiltonian for the non-interacting ($U_i = 0$) electrodes can be expressed as

$$H_{\text{lead}} = \sum_p \epsilon_0 c_p^{\dagger} c_p + \sum_{\langle pq\rangle} t_0\left(c_p^{\dagger} c_q + c_q^{\dagger} c_p\right) \tag{2}$$

with site energy and nearest-neighbor intersite coupling ϵ_0 and t_0, respectively. These electrodes are directly coupled to the 1D chain through the lattice sites 1 and N. The hopping integrals between the source and chain and between the chain and drain are denoted by τ_S and τ_D, respectively.

In the generalized HF approach [25–29], the full Hamiltonian is decoupled into its up-spin and down-spin components by replacing the interaction terms by their mean field (MF) counterparts. This redefines the on-site energies as $\epsilon'_{i\uparrow} = \epsilon_{i\uparrow} + U\langle n_{i\downarrow}\rangle$ and $\epsilon'_{i\downarrow} = \epsilon_{i\downarrow} + U\langle n_{i\uparrow}\rangle$ where, $n_{i\sigma} = c_{i\sigma}^{\dagger} c_{i\sigma}$ is the number operator. With these site energies, the full Hamiltonian (Eq. (1)) can be written in the MF approximation in the decoupled form

$$\begin{aligned} H_{\text{MF}} &= \sum_i \epsilon'_{i\uparrow} n_{i\uparrow} + \sum_{\langle ij\rangle} t\left[c_{i\uparrow}^{\dagger} c_{j\uparrow} + c_{j\uparrow}^{\dagger} c_{i\uparrow}\right] \\ &\quad + \sum_i \epsilon'_{i\downarrow} n_{i\downarrow} + \sum_{\langle ij\rangle} t\left[c_{i\downarrow}^{\dagger} c_{j\downarrow} + c_{j\downarrow}^{\dagger} c_{i\downarrow}\right] \\ &\quad - \sum_i U_i \langle n_{i\uparrow}\rangle\langle n_{i\downarrow}\rangle \\ &= H_{C,\uparrow} + H_{C,\downarrow} - \sum_i U_i \langle n_{i\uparrow}\rangle\langle n_{i\downarrow}\rangle \end{aligned} \tag{3}$$

where, $H_{C,\uparrow}$ and $H_{C,\downarrow}$ correspond to the effective TB Hamiltonians for the up and down spin electrons, respectively. The last term provides a shift in the total energy that depends on the mean populations of the up and down spin states.

With these decoupled Hamiltonians ($H_{C,\uparrow}$ and $H_{C,\downarrow}$) of up and down spin electrons, we start our self consistent procedure considering initial guess values of $\langle n_{i\uparrow}\rangle$ and $\langle n_{i\downarrow}\rangle$. For these initial set of values of $\langle n_{i\uparrow}\rangle$ and $\langle n_{i\downarrow}\rangle$, we numerically diagonalize the up and down spin Hamiltonians. Then we calculate a new set of values of $\langle n_{i\uparrow}\rangle$ and $\langle n_{i\downarrow}\rangle$. These steps are repeated until a self consistent solution is achieved.

The converged mean field Hamiltonian is a sum of single electron up and down spin Hamiltonians. The transmission function is therefore a sum $T(E) = \sum_\sigma T_\sigma(E)$ where [30] $T_\sigma = \text{Tr}[\Gamma_S G^r_{C,\sigma} \Gamma_D G^a_{C,\sigma}]$. Here, $G^r_{C,\sigma}$ and $G^a_{C,\sigma}$ are the retarded and advanced Green's functions, respectively, of the chain including the effects of the electrodes. $G_{C,\sigma} = (E - H_{C,\sigma} - \Sigma_S - \Sigma_D)^{-1}$, where Σ_S and Σ_D are the self-energies due to coupling of the chain to the source and drain, respectively, while Γ_S and Γ_D are their imaginary parts.

3. Results and discussion

In what follows we limit ourselves to absolute zero temperature and use the units where $c = h = e = 1$. For the numerical calculations we choose $t = 1$, $\epsilon_0 = 0$, $t_0 = 3$ and $\tau_S = \tau_D = 1$. The energy scale is measured in unit of t.

Before addressing the central problem, i.e., the possibility of getting multiple mobility edges in 1D superlattice geometries, first we explore the effect of finite bias on electron transport in two simple systems, one for a standard non-interacting chain and the other for a conventional Hubbard chain where all sites are interacting.

In Fig. 3 we show the variation of total transmission probability (T) together with the average density of states as a function

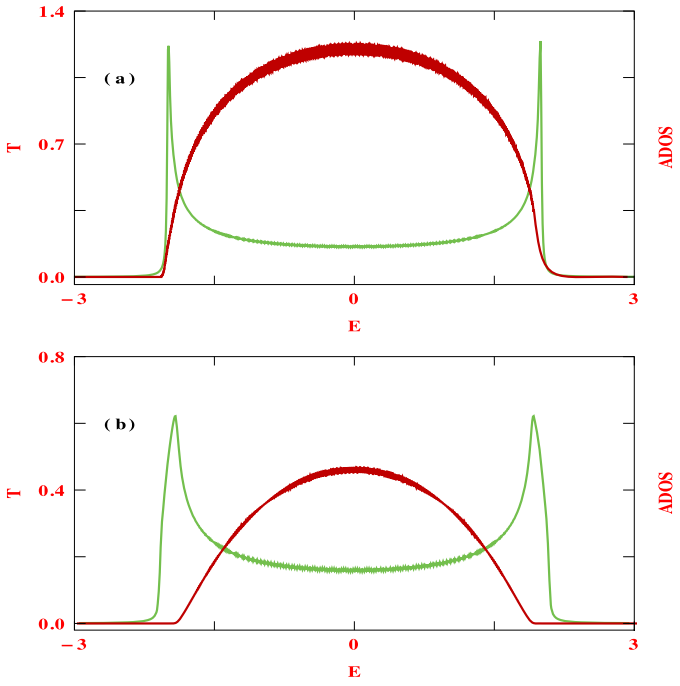

Fig. 3. (Color online.) Transmission probability T (red color) and ADOS (green color) as a function of energy E for a 1D non-interacting ($U_i = 0\ \forall i$) ordered ($W = 0$) chain with $N = 300$ sites. The electrostatic potential profile varies linearly (red curve in Fig. 2), with the total potential drop across the chain to be (a) $V = 0$ and (b) $V = 0.2$.

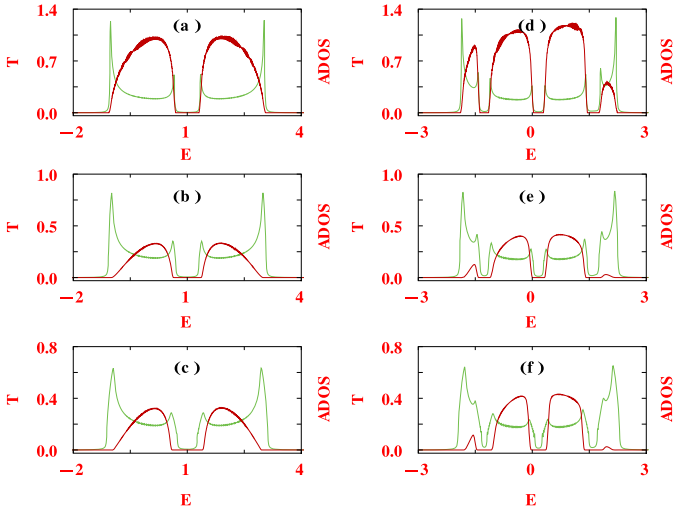

Fig. 4. (Color online.) Transmission probability T (red color) and ADOS (green color) as a function of energy E for an ordered ($W = 0$) 1D chain. The left column corresponds to the case where all sites are interacting ($U_i = 2$), while the right column represents the results for a 1D superlattice geometry where four non-interacting ($U_i = 0$) atoms are placed between two interacting ($U_i = 2$) atoms. The 1st, 2nd and 3rd rows correspond to $V = 0$, 0.1 and 0.2, respectively. All these results are shown for a linear bias drop along the chain.

of energy E for an ordered ($\epsilon_i^0 = 0$ for all atomic sites i in the chain) non-interacting chain for two different magnitudes of the voltage bias, assuming a linear bias drop (uniform electric field) across the chain. In the absence of electric field electron transmission takes place throughout the energy band as clearly seen from the spectrum Fig. 3(a), since in this case all the energy eigenstates are extended. On the other hand, when a finite bias drop takes place along the chain, several energy eigenstates appear in the energy regions around the band edges for which the transmission probability is exactly zero (Fig. 3(b)). Therefore, the chain appears insulating when Fermi energy is within the zone of zero transmission, while finite transmission, $T \neq 0$, is seen more towards the band centre. The sharp transition between these regimes illustrates the existence of a mobility edge phenomenon under finite bias condition. For a finite bias, the localization of energy levels always starts from the band edges and the width of the localized energy zones can be controlled by the imposed electric field. Obviously, for strong enough electric field almost all the energy levels are localized and the extended energy regions disappear, so that in this particular case metal–insulator (MI) transition will no longer be observed. This localization phenomenon in presence of an external electric field has already been established in the literature, but the central issue of our present investigation – the interplay between the Hubbard interaction strength, the superlattice configuration and the electric field has not been addressed earlier.

To explore it, we present in Fig. 4 the results of a traditional Hubbard chain where all sites are interacting (left column) together with the results of a superlattice geometry where four non-interacting atoms are placed between two interacting atoms (right column). The results are shown for three different values of the voltage bias, taking a linear bias drop along the 1D chain. For the chain where all sites are interacting a single energy gap only appears at the band centre, while in the superlattice geometry, depending on the unit cell configuration, multiple energy gaps are generated which are clearly visible from the ADOS spectra. Therefore, in a superlattice geometry, in presence of external electric field associated with bias voltage V between two electrodes, zero transmission ($T = 0$) energy regions exist, and are separated by regions of extended states compared to the traditional Hubbard chain, and, it leads to the possibility of getting an MI-like transition at multiple energies.

The total number of energy sub-bands in a superlattice geometry for a particular energy range generated in the ADOS profile strongly depends on structural details, i.e., the number M of non-interacting atoms between two interacting lattice sites. This is shown in Figs. 5 and 6 which show the ADOS and the transmission probability for two models that are identical in all details (see caption to Fig. 5) except that $M = 5$ in Fig. 5 and $M = 6$ in Fig. 6. These structures show more mobility edge phenomena, that is crossovers between fully opaque and a transmitting zone, than in the corresponding case of Fig. 4(f), suggesting a design concept based on such superlattice structures as a switching devices at multiple energies.

The robustness of the observed behavior can be examined by its sensitivity to the presence of disorder. Fig. 7 displays the ADOS spectrum and the total transmission probability for a 1D chain in presence of diagonal disorder affected by choosing ϵ_i^0 from a uniform distribution of width $W = 0.5$ (-0.25 to $+0.5$). An average over 50 disorder configurations is presented. The resulting ADOS and transmission show similar qualitative features, with sharp transitions between localized and extended spectral regions as seen above for the ordered cases. Note that the presence of disorder alone can cause state localization. For strong enough disorder almost all energy levels get localized, even for such a finite size 1D chain. In this limit such crossover behavior will no longer be observed.

In the calculations presented so far we have assumed a linear drop of the electrostatic potential along the chain. Figs. 8 and 9 show results obtained for an identical chain length with other potential profiles that are characteristics of stronger screening. We see that the localized region gradually decreases with increasing flatness of the potential profile in the interior of the conducting bridge. If the potential drop takes place only at the chain-to-electrode interfaces, i.e., when the potential profile becomes almost flat along the chain the width of the localized region almost

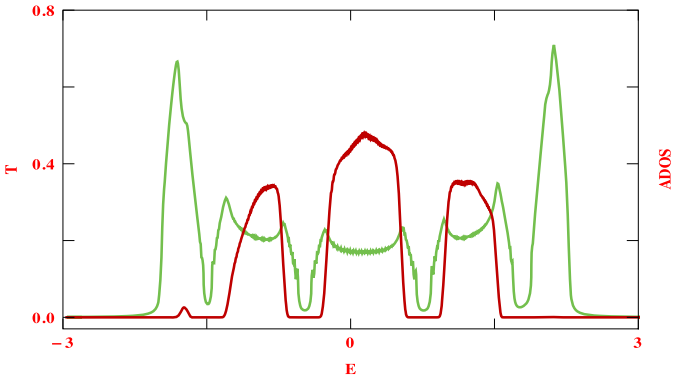

Fig. 5. (Color online.) Transmission probability T (red color) and ADOS (green color) as a function of energy E for a 1D chain ($N = 300$) in absence of disorder ($W = 0$) with on-site interaction $U_i = 2$ and bias voltage $V = 0.2$ that varies linearly along the chain. Here we set $M = 5$, i.e., five non-interacting atoms are placed between two interacting atoms.

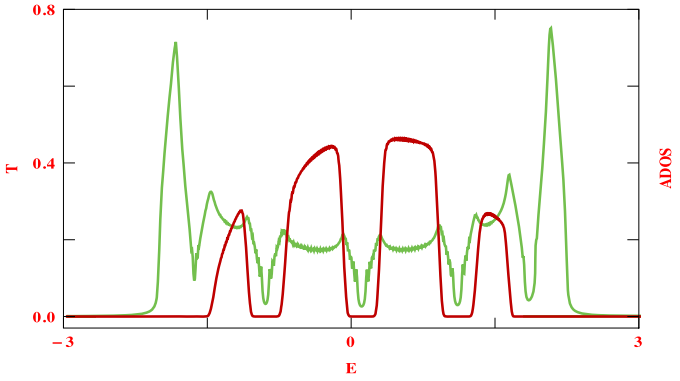

Fig. 6. (Color online.) Same as Fig. 5, with $M = 6$.

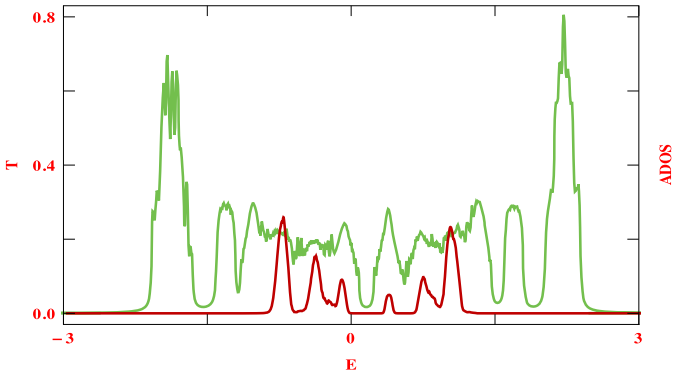

Fig. 7. (Color online.) Transmission probability T (red color) and ADOS (green color) as a function of energy E for a 1D chain ($N = 300$) in presence of disorder ($W = 0.5$) for the same parameter values used in Fig. 4(f): $U_i = 2$, $V = 0.2$ (linear potential profile) and $M = 4$.

vanishes and the metal–insulator transition is not observed, as was the case for the zero bias limit.

Finally, we point out that by locating the Fermi energy in appropriate places of the sub-bands, the system can be used as a p-type or an n-type semiconductor. For example, let us imagine, at absolute zero temperature, the Fermi level is fixed in the localized region which is very close to the fully transmitting zone (right-hand side). In this case, the left sub-bands up to the Fermi level are completely filled with electrons. Now, if the energy gap between the Fermi level, pinned in the localized region, and the bottom of the transmitting region (right-hand side) is small enough for electrons to hop, then the system will behave as an n-type

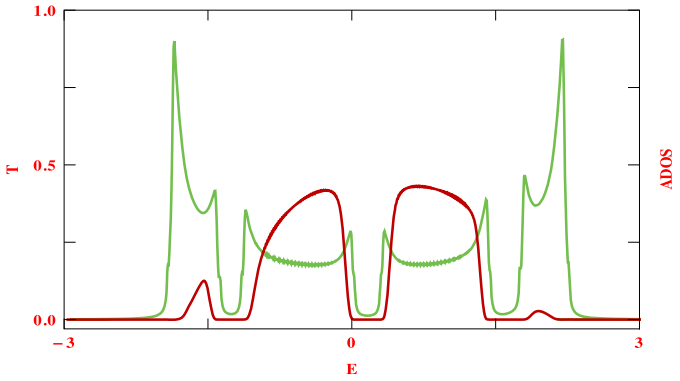

Fig. 8. (Color online.) Transmission probability T (red color) and ADOS (green color) as a function of energy E for a 1D chain ($N = 300$) with no disorder ($W = 0$). The model parameters are $U = 2$, $M = 4$ and $V = 0.2$, with the bias potential profile taken as the green curve given of Fig. 2.

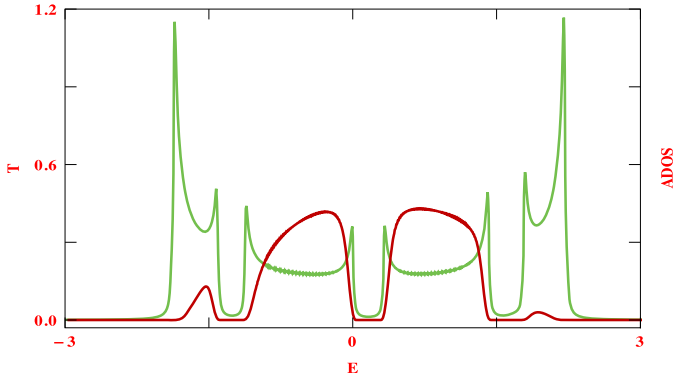

Fig. 9. (Color online.) Same as Fig. 8, with the electrostatic potential profile given by the blue curve in Fig. 2.

semiconductor. On the other hand, by reverting the situation we can generate a p-type semiconductor where electrons hop from a filled transmitting zone (valence band) to unoccupied localized zone (conduction band) generating holes in the valence band.

4. Conclusion

To summarize, we have investigated in detail the two-terminal finite bias electron transport in a 1D superlattice structure composed of interacting and non-interacting atoms. The electron–electron interaction is considered in the Hubbard form, and the Hamiltonian is solved within a generalized HF scheme. We numerically calculate two-terminal transport by using a Green's function formalism and analyze the results for some specific chain structures characterized by different arrangements of the atomic sites in the chain. Our analysis may be utilized in designing a tailor made switching device for multiple values of Fermi energy (or, more practically, for different values of a gating potential). The sensitivity of this switching action, i.e., metal-to-insulator transition and vice versa on the electric field variation has also been discussed. Though the results presented in this Letter are worked out at absolute zero temperature limit, the results should remain valid even at finite temperatures (~ 300 K) since the broadening of the energy levels of the superlattice structure due to its coupling with the metal electrodes is much higher than that of the thermal broadening [31–34].

Acknowledgements

The research of A.N. is supported by the Israel Science Foundation, the Israel–US Binational Science Foundation, the European

Research Council under the European Union's Seventh Framework Program (FP7/2007-2013; ERC Grant No. 226628) and the Israel–Niedersachsen Research Fund.

References

[1] P.W. Anderson, Phys. Rev. 109 (1958) 1492.
[2] G.H. Wannier, Phys. Rev. 117 (1960) 432.
[3] D.H. Dunlap, H.-L. Wu, P. Phillips, Phys. Rev. Lett. 65 (1990) 88.
[4] A. Sánchez, E. Maciá, F. Domínguez-Adame, Phys. Rev. B 49 (1994) 147.
[5] F.A.B.F. de Moura, M.L. Lyra, Phys. Rev. Lett. 81 (1998) 3735.
[6] F.M. Izrailev, A.A. Krokhin, Phys. Rev. Lett. 82 (1999) 4062.
[7] F. Domínguez-Adame, V.A. Malyshev, F.A.B.F. de Moura, M.L. Lyra, Phys. Rev. Lett. 91 (2003) 197402.
[8] S. Aubry, G. André, in: L. Horwitz, Y. Neeman (Eds.), Group Theoretical Methods in Physics, Annals of the Israel Physical Society, vol. 3, American Institute of Physics, New York, 1980, p. 133.
[9] S. Sil, S.K. Maiti, A. Chakrabarti, Phys. Rev. B 79 (2009) 193309.
[10] C.M. Soukoulis, E.N. Economou, Phys. Rev. Lett. 48 (1982) 1043.
[11] S. Das Sarma, S. He, X.C. Xie, Phys. Rev. Lett. 61 (1988) 2144.
[12] M. Johansson, R. Riklund, Phys. Rev. B 42 (1990) 8244.
[13] A. Eilmes, R.A. Römer, M. Schreiber, Eur. Phys. J. B 23 (2001) 229.
[14] S. Sil, S.K. Maiti, A. Chakrabarti, Phys. Rev. Lett. 101 (2008) 076803.
[15] S. Sil, S.K. Maiti, A. Chakrabarti, Phys. Rev. B 78 (2008) 113103.
[16] T. Paiva, R.R. dos Santos, Phys. Rev. Lett. 76 (1996) 1126.
[17] T. Paiva, R.R. dos Santos, Phys. Rev. B 58 (1998) 9607.
[18] T. Paiva, R.R. dos Santos, Phys. Rev. B 62 (2000) 7007.
[19] T. Paiva, R.R. dos Santos, Phys. Rev. B 65 (2002) 153101.
[20] C. -bo Duan, W.-Z. Wang, J. Phys.: Condens. Matter 22 (2010) 345601.
[21] B. Heinrich, J.F. Cochran, Adv. Phys. 42 (1993) 523.
[22] P. Grünberg, S. Demokritov, A. Fuss, M. Vohl, J.A. Wolf, J. Appl. Phys. 69 (1991) 4789.
[23] S.S.P. Parkin, N. More, K.P. Roche, Phys. Rev. Lett. 64 (1990) 2304.
[24] J. Chowdhury, S.N. Karmakar, B. Bhattacharyya, Phys. Rev. B 75 (2007) 235117.
[25] S.K. Maiti, A. Chakrabarti, Phys. Rev. B 82 (2010) 184201.
[26] S.K. Maiti, Solid State Commun. 150 (2010) 2212.
[27] S.K. Maiti, Phys. Status Solidi B 248 (2011) 1933.
[28] H. Kato, D. Yoshioka, Phys. Rev. B 50 (1994) 4943.
[29] A. Kambili, C.J. Lambert, J.H. Jefferson, Phys. Rev. B 60 (1999) 7684.
[30] M. Cini, Phys. Rev. B 22 (1980) 5887.
[31] S.K. Maiti, Solid State Commun. 149 (2009) 973.
[32] S.K. Maiti, Phys. Scr. 75 (2007) 62.
[33] S.K. Maiti, Physica B 394 (2007) 33.
[34] S. Datta, Electronic Transport in Mesoscopic Systems, Cambridge University Press, Cambridge, 1997.